

Simplified analysis for the initial design of rectangular waveguide cross-slot couplers

K. Rambabu, H.A. Thiart and J. Bornemann

Abstract: For the purpose of providing initial designs of waveguide cross-slot couplers, the authors present a simplified analysis of cross-slot coupling through the common broad wall of two rectangular waveguides. Straightforwardly implementable equations are presented which not only include a wide range of cross-slot dimensions but also the location as well as the rotation of the cross-slot in a coupler environment. Moreover, asymmetric coupler structures can be easily incorporated. Analyses of individual structures are verified by HFSS. Two examples of cross-slot waveguide couplers demonstrate the applicability of this technique for the initial design of waveguide cross-slot couplers.

1 Introduction

The standard design process for passive microwave components consists of an initial design followed by a full-wave analysis and optimisation. It is well known that the design cycle is shortened considerably if an initial design, which is close to the desired performance, can be obtained quickly, e.g. via equivalent circuits or closed-form expressions, and without the use of electromagnetic field solvers.

An initial design for a waveguide coupler usually involves Bethe's coupling theory [1] and other data such as measurements performed on certain apertures, e.g. [2, 3]. To streamline the design process of aperture couplers, functional approximations to the polarisabilities of a number of different coupling apertures, such as rectangle, circle, diamond, rounded-end slot, ellipse, etc, have been developed and reported in the literature, e.g. [4-9]. However, although cross-slot couplers have been used for a long time, e.g. [10, 11], none of these references present functional solutions for the initial design of cross-slot apertures.

Another approach to design cross-slot couplers consists in utilising field solvers right from the beginning. However, since the theoretical computation of the aperture is mathematically complex, e.g. [12], or, alternatively, requires considerable CPU time with a field solver to develop design guidelines for various dimensions, this approach leads to prohibitively long prototype developments in many practical applications.

The cross-slot is one of the important apertures in coupler design and is also frequently employed in filters and antenna feed systems, e.g. [13, 14]. However, to the best of the authors' knowledge, closed-form expressions for the electric and magnetic polarisabilities of cross-slots (and especially ones with rounded corners) have not been reported. So far, only measured polarisabilities are available for this aperture [2, 3].

Therefore, this paper focuses on an initial design concept for cross-slot couplers, including a simplified analysis, for the purpose of facilitating a speedy design process. For the first time in the literature, the measured data for the cross-slot polarisabilities in [2, 3] are curve fitted. Larger cross-slots are analysed by field averaging, which has been demonstrated, but only for rectangular and circular apertures, in [15]. Then, by utilising concepts similar to those in [16], a fairly simple strategy for the initial design and simplified analysis of E-plane waveguide cross-slot couplers is developed. Moreover, this approach includes the effect of the orientation of the slot and allows coupling between asymmetric waveguides.

2 Theory

2.1 Small cross-slot

Figure 1 shows the E-plane waveguide coupler with a cross-slot in the common broad wall.

Assuming monomode propagation, the electromagnetic field incident at port 1 can be written as

$$E_y = \sin\left(\frac{\pi x}{a}\right)e^{-j\beta z} \quad (1)$$

$$H_x = -\frac{1}{Z} \sin\left(\frac{\pi x}{a}\right)e^{-j\beta z} \quad (2)$$

$$H_z = \frac{j\pi}{\beta a Z} \cos\left(\frac{\pi x}{a}\right)e^{-j\beta z} \quad (3)$$

where βz is the phase term in axial direction, and Z is the wave impedance of the fundamental mode.

Using the reciprocity theorem [17], the forward (C^F) and reverse (C^R) coupling coefficients can be written as

$$C^F = \frac{-j\omega}{P_1} \left[\varepsilon_0 \alpha_e \sin^2\left(\frac{\pi h}{a}\right) - \frac{\mu_0 \alpha_m}{Z^2} \left[\sin^2\left(\frac{\pi h}{a}\right) + \frac{\pi^2}{\beta^2 a^2} \cos^2\left(\frac{\pi h}{a}\right) \right] \right] \quad (4)$$

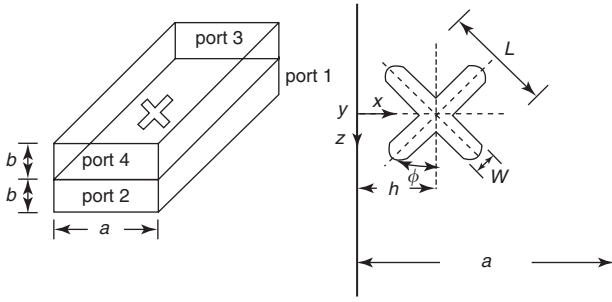


Fig. 1 *E*-plane waveguide coupler with a cross-slot in the common broad wall
The cutter radius is $W/2$

$$C^R = \frac{-j\omega}{P_1} \left[\varepsilon_0 \alpha_e \sin^2 \left(\frac{\pi h}{a} \right) + \frac{\mu_0 \alpha_m}{Z^2} \left[\sin^2 \left(\frac{\pi h}{a} \right) - \frac{\pi^2}{\beta^2 a^2} \cos^2 \left(\frac{\pi h}{a} \right) \right] \right] \quad (5)$$

where $P_1 = ab/Z$, and α_e and α_m are the electric and magnetic polarisabilities of the cross-slot. By curve fitting the measurements in [2, 3] using a least square method, the following closed-form expressions for the polarisabilities of the cross-slot are obtained.

$$\alpha_e = 10^{-2} L^3 \left[-411.5266 \left(\frac{W}{L} \right)^5 + 261.1877 \left(\frac{W}{L} \right)^4 - 87.8896 \left(\frac{W}{L} \right)^3 + 46.68 \left(\frac{W}{L} \right)^2 + 0.1901 \left(\frac{W}{L} \right) - 0.0007 \right] \quad 0.1 < \frac{W}{L} \leq 0.35 \quad (6)$$

$$\alpha_m = 10^{-2} L^3 \left[2.86 + 36.16 \left(\frac{W}{L} \right) - 50.22 \left(\frac{W}{L} \right)^2 + 41.39 \left(\frac{W}{L} \right)^3 - 13.54 \left(\frac{W}{L} \right)^4 \right] \quad 0.1 < \frac{W}{L} \leq 1 \quad (7)$$

Similarly, the scattered fields in the input waveguide can be written as

$$S^F = \frac{j\omega}{P_1} \left[\varepsilon_0 \alpha_e \sin^2 \left(\frac{\pi h}{a} \right) - \frac{\mu_0 \alpha_m}{Z^2} \left[\sin^2 \left(\frac{\pi h}{a} \right) + \frac{\pi^2}{\beta^2 a^2} \cos^2 \left(\frac{\pi h}{a} \right) \right] \right] \quad (8)$$

$$S^R = \frac{j\omega}{P_1} \left[\varepsilon_0 \alpha_e \sin^2 \left(\frac{\pi h}{a} \right) + \frac{\mu_0 \alpha_m}{Z^2} \left[\sin^2 \left(\frac{\pi h}{a} \right) - \frac{\pi^2}{\beta^2 a^2} \cos^2 \left(\frac{\pi h}{a} \right) \right] \right] \quad (9)$$

With (4), (5), (8) and (9), the S-parameters of the coupler can be represented by

$$S_{11} = 20 \log |S^R| \quad (10)$$

$$S_{31} = 20 \log |C^R| \quad (11)$$

$$S_{41} = 20 \log |C^F| \quad (12)$$

$$S_{21} = 10 \log (1 - |C^F|^2 - |C^R|^2 - |S^R|^2) \quad (13)$$

The above expressions are simple and can be straightforwardly implemented. To verify the basic approach, Fig. 2 shows a direct comparison of this approach with results obtained by HFSS using a slot thickness of $25.4 \mu\text{m}$. Although slight differences can be observed in the forward (S_{41}) and reverse (S_{31}) coupling performance, the general agreement is good—considering the simplicity of the model—and, therefore, appears feasible in an initial design task. Note that according to the simplified approach used here, the reverse coupling (S_{31}) always equals the input reflection coefficient (S_{11}) whereas there is a slight difference between them in HFSS due to finite wall thickness.

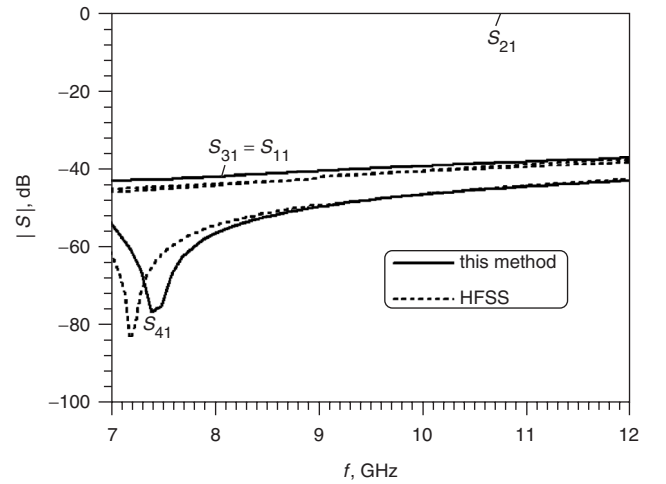


Fig. 2 Comparison of results of this method (solid lines) and HFSS (dashed lines) for a small cross-slot (cf. Fig. 1)
Dimensions: $a = 22.86 \text{ mm}$, $b = 10.16 \text{ mm}$, $L = 5 \text{ mm}$, $w = 1.5 \text{ mm}$, $h = a/2$, $\phi = 0^\circ$

2.2 Large cross-slot

Apertures in coupling applications frequently assume a larger size than that permitted by Bethe's coupling theory [1]. To include larger cross-slot apertures in the initial coupler design process, the fields averaged over the aperture are considered in the analysis rather than those at the aperture center for small cross-slots [15].

Assuming that the width of the slot is small enough to produce a constant field, then the normalised field averaged over the length of the slot can be represented by

$$E_y^{avg} = \frac{1}{2L} \left[\int_{-L/2}^{L/2} \sin \frac{\pi}{a} (h - \rho \sin \phi) e^{-j\beta \rho \cos \phi} d\rho + \int_{-L/2}^{L/2} \sin \frac{\pi}{a} (h + \rho \cos \phi) e^{-j\beta \rho \sin \phi} d\rho \right] \\ = \frac{2}{M^2 + N^2} \left[\sin \left(\frac{ML}{2} \right) \cosh \left(\frac{NL}{2} \right) \left(M \sin \left(\frac{\pi h}{a} \right) - N \cos \left(\frac{\pi h}{a} \right) \right) + \cos \left(\frac{ML}{2} \right) \sinh \left(\frac{NL}{2} \right) \left(N \sin \left(\frac{\pi h}{a} \right) + M \cos \left(\frac{\pi h}{a} \right) \right) \right] \\ + \frac{2}{P^2 + Q^2} \left[\sin \left(\frac{PL}{2} \right) \cosh \left(\frac{QL}{2} \right) \left(P \sin \left(\frac{\pi h}{a} \right) + Q \cos \left(\frac{\pi h}{a} \right) \right) + \cos \left(\frac{PL}{2} \right) \sinh \left(\frac{QL}{2} \right) \left(Q \sin \left(\frac{\pi h}{a} \right) - P \cos \left(\frac{\pi h}{a} \right) \right) \right] \quad (14)$$

The H_x component is obtained from $H_x^{avg} = -(1/Z)E_y^{avg}$, and averaging the H_z component leads to

$$H_z^{avg} = \frac{A}{2L} \left[\int_{-L/2}^{L/2} \cos \frac{\pi}{a} (h - \rho \sin \phi) e^{-j\beta\rho \cos \phi} d\rho + \int_{-L/2}^{L/2} \cos \frac{\pi}{a} (h + \rho \cos \phi) e^{-j\beta\rho \sin \phi} d\rho \right]$$

$$= \frac{2A}{M^2 + N^2} \left[\sin \left(\frac{ML}{2} \right) \cosh \left(\frac{NL}{2} \right) \left(M \cos \left(\frac{\pi h}{a} \right) + N \sin \left(\frac{\pi h}{a} \right) \right) + \cos \left(\frac{ML}{2} \right) \sinh \left(\frac{NL}{2} \right) \left(N \cos \left(\frac{\pi h}{a} \right) - M \sin \left(\frac{\pi h}{a} \right) \right) \right]$$

$$+ \frac{2A}{P^2 + Q^2} \left[\sin \left(\frac{PL}{2} \right) \cosh \left(\frac{QL}{2} \right) \left(P \cos \left(\frac{\pi h}{a} \right) - Q \sin \left(\frac{\pi h}{a} \right) \right) + \cos \left(\frac{PL}{2} \right) \sinh \left(\frac{QL}{2} \right) \left(Q \cos \left(\frac{\pi h}{a} \right) + P \sin \left(\frac{\pi h}{a} \right) \right) \right] \quad (15)$$

The remaining quantities in (14), (15) are given by

$$A = \frac{j\pi}{\beta a Z}; \quad M = \frac{\pi}{a} \sin \phi; \quad N = -j\beta \cos \phi;$$

$$P = \frac{\pi}{a} \cos \phi; \quad Q = -j\beta \sin \phi \quad (16)$$

The coupled fields in forward and reverse direction can then be estimated from

$$C^F = -\frac{j\omega}{P_1} \left[\varepsilon_0 \alpha_e E_{avg}^y \sin \left(\frac{\pi h}{a} \right) + \mu_0 \alpha_m \left\{ -\frac{1}{Z^2} E_{avg}^y \sin \left(\frac{\pi h}{a} \right) + \frac{j\pi}{\beta a Z} H_{avg}^z \cos \left(\frac{\pi h}{a} \right) \right\} \right] \quad (17)$$

$$C^R = -\frac{j\omega}{P_1} \left[\varepsilon_0 \alpha_e E_{avg}^y \sin \left(\frac{\pi h}{a} \right) + \mu_0 \alpha_m \left\{ \frac{1}{Z^2} E_{avg}^y \sin \left(\frac{\pi h}{a} \right) + \frac{j\pi}{\beta a Z} H_{avg}^z \cos \left(\frac{\pi h}{a} \right) \right\} \right] \quad (18)$$

Since S_{11} equals S_{31} , (17) and (18) are sufficient to compute the four scattering parameters according to (10)–(13).

At the example of a moderately large cross-slot, Fig. 3 shows a comparison between results obtained with this

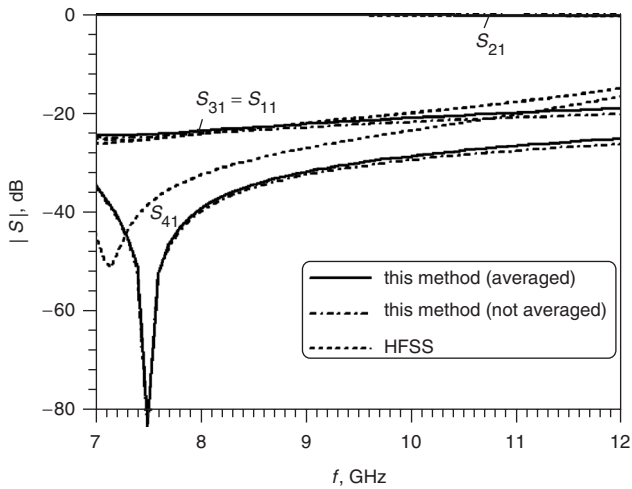


Fig. 3 Comparison of results of this method with (solid lines) and without (dash-dotted lines) field averaging and HFSS (dashed lines) for the structure in Fig. 1

Dimensions: $a = 22.86$ mm, $b = 10.16$ mm, $L = 10$ mm, $w = 2.5$ mm, $h = a/2$, $\phi = 0^\circ$

method (both with and without field averaging) and HFSS. First of all, the agreement with HFSS is good with the field-averaged solutions slightly closer to the HFSS results. Secondly, there is only a slight discrepancy between the results with direct and averaged fields. As the slot dimensions increase, so does the difference between these two approaches, up to a point where the direct-field approach yields non-physical solutions ($|S_{21}| > 1$) in (13). The field-averaged solution continues to provide reasonable data with increasing cross-slot size but at the expense of increasing disagreement with HFSS. This is, of course, an expected tendency as aperture resonance effects are not included in the simplified model.

2.3 Coupling between different waveguides

One of the advantages of this approach is the fact that contrary to common coupler design utilising even and odd modes, e.g. [18], the coupled waveguides need not be of the same size. The inset in Fig. 4 shows the arrangement of two different waveguides coupled through a cross-slot. By applying an analysis similar to that of Section 2.1, we can write the coupling coefficients in forward and reverse directions as follows

$$C^F = \frac{-j\omega}{P_2} \left[\varepsilon_0 \alpha_e \sin \left(\frac{\pi D}{a_2} \right) \sin \left(\frac{\pi h}{a_1} \right) - \frac{\mu_0 \alpha_m}{Z_1 Z_2} \left[\sin \left(\frac{\pi D}{a_2} \right) \sin \left(\frac{\pi h}{a_1} \right) + \frac{\pi^2}{\beta_1 \beta_2 a_1 a_2} \cos \left(\frac{\pi D}{a_2} \right) \cos \left(\frac{\pi h}{a_1} \right) \right] \right] \quad (19)$$

$$C^R = \frac{-j\omega}{P_2} \left[\varepsilon_0 \alpha_e \sin \left(\frac{\pi D}{a_2} \right) \sin \left(\frac{\pi h}{a_1} \right) + \frac{\mu_0 \alpha_m}{Z_1 Z_2} \left[\sin \left(\frac{\pi D}{a_2} \right) \sin \left(\frac{\pi h}{a_1} \right) - \frac{\pi^2}{\beta_1 \beta_2 a_1 a_2} \cos \left(\frac{\pi D}{a_2} \right) \cos \left(\frac{\pi h}{a_1} \right) \right] \right] \quad (20)$$

where $Z_1 = \omega\mu_0/\beta_1$, $Z_2 = \omega\mu_0/\beta_2$, $P_2 = a_2 b_2/Z_2$, $D = h - (a_1 - a_2)/2$, and β_1 , β_2 are the propagation constants for the TE₁₀ modes in the respective waveguides.

As an example, Fig. 4 shows a comparison of this theory with HFSS. Although there are differences between the two

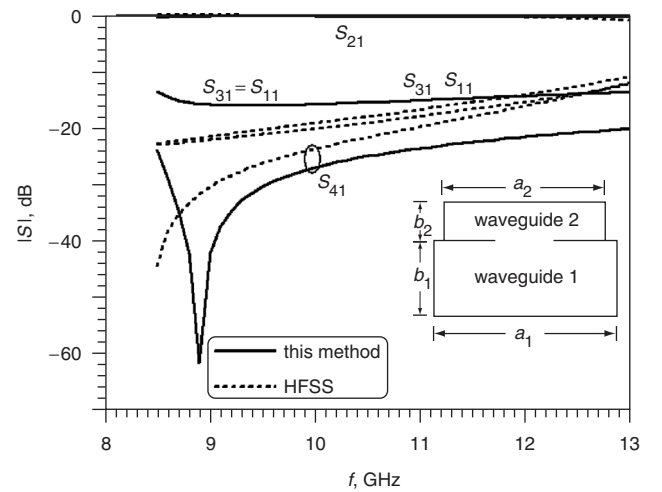


Fig. 4 Cross-slot coupling between two different waveguides and comparison with results from HFSS

Dimensions: $a_1 = 22.86$ mm, $b_1 = 10.16$ mm, $a_2 = 18$ mm, $b_2 = 8$ mm, $L = 10$ mm, $w = 2.55$ mm, $h = a/2$, $\phi = 0^\circ$

sets of curves, it is obvious that this approach provides sufficient accuracy to be used as an initial design procedure.

3 Design examples

In this Section, we demonstrate that couplers with given specifications can be initially designed using the above analysis.

For simplicity, we assume uniformly spaced identical cross-slot apertures. (Different apertures and aperture spacings can be accounted for using the procedure in [16]). The coupling due to multiple slots, which are unevenly placed in the common wall between two rectangular waveguides of propagation constants β_1 and β_2 , can be written as

$$C_{Total}^R = C_s^R \sum_{i=1}^N e^{-j(\beta_1 + \beta_2)d_{i1}} \quad (21)$$

$$C_{Total}^F = C_s^F \sum_{i=1}^N e^{-j(\beta_1 d_{i1} + \beta_2 d_{iN})} \quad (22)$$

where C_s^R and C_s^F are the reverse and forward coupling, respectively, due to a single cross-slot; d_{ij} are the distances between the i th slot and j th slot with $d_{ii} = 0$.

To demonstrate the validity of our approach for the initial design of waveguide cross-slot couplers, which need not necessarily be directional couplers, we assume in this example a backward coupling (C_{Total}^R) of 20 dB at an operating frequency of 10 GHz in WR90 waveguides. If the design aims for smallest aperture dimensions and maximum reverse coupling, then the distances between the apertures should be approximately $\lambda_g/2$. (Depending on the specific application with respect to forward and backward coupling, the spacing between the apertures can be adjusted.) The only unknown in (21) is now the dimension of the slot. Figure 5 shows the initial design using this method with three apertures (solid lines) and compares it to the results of an HFSS analysis (dashed lines). The design goal of 20 dB reverse coupling at 10 GHz is achieved exactly, and the forward coupling is almost 10 dB lower (29.9 dB). The respective HFSS values are 21.5 dB and 26.7 dB. Note that the agreement is reasonable over a wider bandwidth and, therefore, allows for an immediate fine optimisation in an actual design scenario.

The last example is a conventional 9 GHz, 20 dB forward directional coupler with three cross-slots and inter-slot distances of somewhat less than $\lambda_g/4$. According to [18], the slots are no longer centered with respect to the waveguide broad wall but are located at $h = a/4$ (cf. Figure 1) and, as additional proof of generality, rotated by $\phi = 45^\circ$. Figure 6 shows the results obtained with this method and with HFSS. Good agreement can be observed for all four S parameters, hence validating the initial design procedure.

Note that since the cross-slot aperture is fairly complex, we expect our initial design to have a slightly higher deviation from the ideal performance than those reported for simple circular or rectangular apertures, e.g. [15]. Nevertheless, Figs. 5 and 6 demonstrate initial designs whose performances are close enough to the specifications so that they can be immediately fine-tuned (without any further investigation) using a field-based analysis method and any optimisation strategy. Thus the initial design guidelines presented here are a very useful contribution to the pool of CAD procedures for waveguide components.

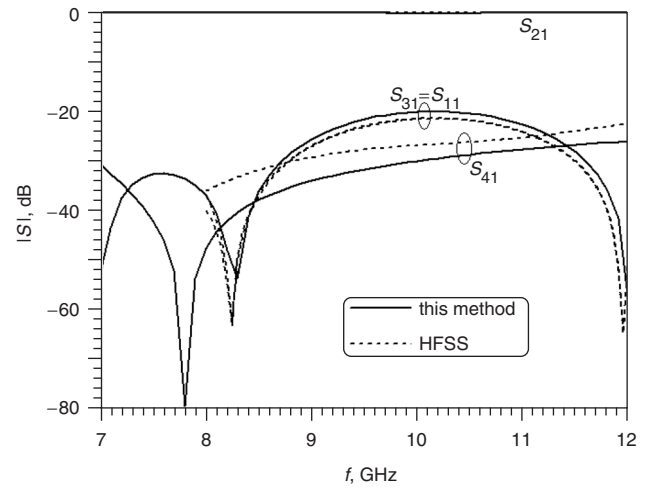


Fig. 5 Initial design of a three-cross-slot 20 dB backward coupler and comparison with results by HFSS

Dimensions: $a = 22.86$ mm, $b = 10.16$ mm, $L = 6.9$ mm, $w = 2.1$ mm, $h = a/2$, $\phi = 0^\circ$, $d = 19.85$ mm

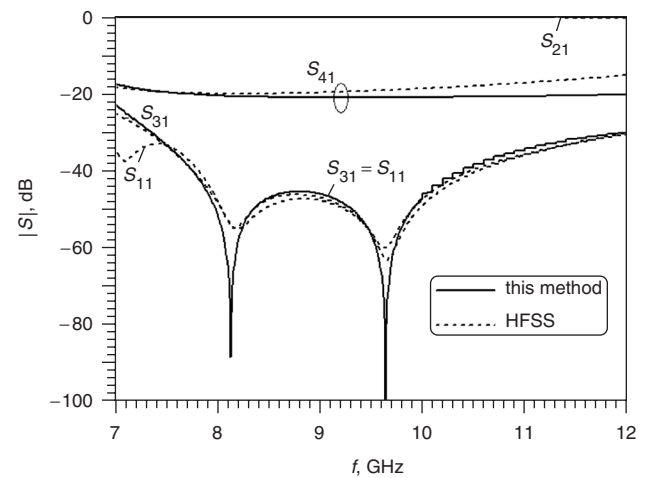


Fig. 6 Initial design of a three-cross-slot 20 dB forward coupler and comparison with results by HFSS

Dimensions: $a = 22.86$ mm, $b = 10.16$ mm, $L = 8.875$ mm, $w = 2.66$ mm, $h = a/4$, $\phi = 45^\circ$, $d = 7.05$ mm

4 Conclusions

The simplified analysis of cross-slot coupling through the common broad wall of two rectangular waveguides provides a useful tool for the initial design of waveguide cross-slot couplers. The closed-form equations presented are easily implemented on a computer even though they include the angular rotation of the slots. Moreover, a wide range of slot dimensions is considered through field averaging, and coupling between different waveguides is included. Two examples with three sets of cross-slot apertures exhibiting different coupling schemes have been presented. Their verification with HFSS demonstrates the usefulness of this technique for the initial design of waveguide cross-slot couplers.

5 References

- 1 Bethe, H.A.: 'Theory of diffraction by small holes', *Phys. Rev.*, 1944, **66**, pp. 163–182
- 2 Cohn, S.B.: 'Determination of aperture parameters by electrolytic-tank measurements', *Proc. IRE*, 1951, **39**, pp. 1416–1421
- 3 Cohn, S.B.: 'The electric polarizability of apertures of arbitrary shape', *Proc. IRE*, 1952, **40**, pp. 1069–1071

- 4 Montgomery, C.G., Dicke, R.H., and Purcell, E.M.: 'Principles of microwave circuits', MIT Rad. Lab. Series (McGraw-Hill, New York, 1948)
- 5 Matthaei, G., Young, L., and Jones, E.M.T.: 'Microwave filters, impedance-matching networks, and coupling structures' (Artech House, Dedham, 1980), chap. 5
- 6 Collin, R.E.: 'Field theory of guided waves' (McGraw-Hill, New York, 1960)
- 7 McDonald, N.A.: 'Polynomial approximations for the electric polarizabilities of some small apertures', *IEEE Trans. Microw. Theory Tech.*, 1985, **33**, pp. 1146–1149
- 8 McDonald, N.A.: 'Polynomial approximations for the transverse magnetic polarizabilities of some small apertures', *IEEE Trans. Microw. Theory Tech.*, 1987, **35**, pp. 20–23
- 9 McDonald, N.A.: 'Simple approximations for the longitudinal magnetic polarizabilities of some small apertures', *IEEE Trans. Microw. Theory Tech.*, 1988, **36**, pp. 1141–1144
- 10 Voss, W.A.G.: 'Optimized crossed-slot directional coupler', *Microw. J.*, 1963, **6**, (5), pp. 83–87
- 11 Meyer, P., and Kruger, J.C.: 'Wideband crossed-waveguide directional couplers'. IEEE Int. Microwave Symp. Dig., Baltimore, USA, June 1998, pp. 253–256
- 12 Jiang, Z., and Shen, Z.: 'Mode-matching analysis of large aperture coupling and its application to the design of waveguide directional couplers', *IEE Proc., Microw. Antennas Propag.*, 2003, **150**, pp. 422–428
- 13 Williams, A.E., and Atia, A.E.: 'Dual-mode canonical waveguide filters', *IEEE Trans. Microw. Theory Tech.*, 1977, **25**, pp. 1021–1026
- 14 Targonski, S.D., and Pozar, D.M.: 'Design of wideband circularly polarized aperture-coupled microstrip antennas', *IEEE Trans. Antennas Propag.*, 1993, **41**, pp. 214–220
- 15 Levy, R.: 'Improved single and multiaperture waveguide coupling theory, including explanation of mutual interactions', *IEEE Trans. Microw. Theory Tech.*, 1980, **28**, pp. 331–338
- 16 Rambabu, K., and Bornemann, J.: 'Analysis and design of profiled multi-aperture stripline-to-microstrip couplers', *IEE Proc., Microw. Antennas Propag.*, 2003, **150**, pp. 484–488
- 17 Collins, R.E.: 'Foundations of microwave engineering' (McGraw-Hill, New York, 1966)
- 18 Uher, J., Bornemann, J., and Rosenberg, U.: 'Waveguide components for antenna feed systems: theory and CAD' (Artech House, Norwood, 1993)